International Journal of Remote Sensing
iFirst, 2011, 1–18

Taylor & Francis
Taylor & Francis Group

Changes in vegetation spring dates in the second half of the twentieth century

JOSÉ A. SOBRINO†, YVES JULIEN*† and LUIS MORALES‡

†Global Change Unit, Image Processing Laboratory, University of Valencia, Spain
‡Departamento de Ciencias Ambientales y Recursos Naturales Renovables, Facultad de Ciencias Agronómicas, Universidad de Chile, A. Santa Rosa 11315, Casilla 1004, Santiago, Chile

(*Received 13 November 2007; in final form 14 May 2010*)

This study aims at estimating trends in spring phenology from vegetation index and air temperature at 2 m height. To this end, we have developed a methodology to infer spring phenological dates from Global Inventory Modeling and Mapping Studies (GIMMS) Normalized Difference Vegetation Index (NDVI) time-series, which are then extrapolated to the period 1948–2006 with the help of Reanalysis data, using its 2 m height air temperature parameter. First, yearly NDVI is fitted to a double-logistic function for the whole extent of the GIMMS database (1981–2003). This fitting procedure allows us to describe, on a yearly basis, the NDVI evolution for each pixel through the estimation of six parameters which include the spring date. Retrieved spring date time-series are then upscaled to Reanalysis database resolution and compared to degree-day amounts. Those degree-day amounts are estimated for various thresholds in order to determine the best thresholds for their calculations on a pixel-by-pixel basis. Once the correct thresholds are identified by correlation with corresponding GIMMS spring date time-series, spring dates are estimated for the whole extent of the Reanalysis database (1948–2006). Finally, Mann–Kendall trend tests are conducted on degree-day-retrieved spring date time-series and trends are estimated only for those pixels that show statistically significant trends. These trends in spring occurrence have an average value of –0.03 days per year, but range between –0.9 and +0.9 days per year, depending on the considered areas. Since the approach is based only on air temperature, retrieved spring dates for vegetation whose growth is limited by water are unreliable, as correlation analysis confirms. The obtained spring date trends show good coherence with previous studies and could be used for climate change impact studies, especially in polar and temperate areas, where the model is more reliable.

1. Introduction

Numerous studies have evidenced the global warming phenomenon (Salinger 2005, IPCC 2007), which can be clearly identified in the evolution of air temperatures over the globe. These are increasing (Salinger 2005), which leads to necessary adaptation

*Corresponding author. Email: yves.julien@uv.es

International Journal of Remote Sensing
ISSN 0143-1161 print/ISSN 1366-5901 online © 2011 Taylor & Francis
http://www.tandf.co.uk/journals
DOI: 10.1080/01431161.2010.496470

of the ecosystems to these new conditions. Since air temperature is one of the parameters on which vegetation regulates its phenological states (other parameters being water, Sun irradiance and nutrient availability), changes in air temperature will lead to changes in vegetation growth, and can lead to a reduction in biodiversity, due to the capacity that some species have to adapt to temperature changes over the ones that cannot (Green *et al*. 2003).

For each vegetal species, all phenological events, such as bud sprouting, flower blooming and senescence, occur at a given moment, which depends on the climate of the previous months. The dependence on surrounding temperature can be modelled with the help of degree-days (Réaumur 1735), calculated from air temperatures at 2 m height. Phenological events occur when given degree-day thresholds are reached, depending on the vegetal species (Snyder *et al*. 1999). Thus, the recent changes in air temperature must be mirrored in the phenological phases of the vegetation, evidencing changes in the vegetal response to their environment (Weber 2001). For example, Sherry *et al*. (2007) showed that an increase in air temperature could result in either an advance or a delay in phenology phases depending on the occurrence of phenological events in relation to summer heat peak timing.

Remotely sensed data are a useful tool for vegetation monitoring, since their global coverage exempts one from tedious ground inventories, and their usefulness has been demonstrated in various studies dedicated to land-cover monitoring (Myneni *et al*. 1997, Tucker *et al*. 2001, Zhou *et al*. 2001, Bogaert *et al*. 2002, Stöckli and Vidale 2004, Chen *et al*. 2005, Beck *et al*. 2006). Currently, the satellite archive for vegetation monitoring covering the longest time period has been derived from the National Oceanic and Atmospheric Administration's (NOAA) satellite series. These satellites carry on board the Advanced Very High Resolution Radiometer (AVHRR) sensor, the data from which have been especially valuable for vegetation monitoring (Myneni *et al*. 1997, Zhou *et al*. 2001, Bogaert *et al*. 2002, Stöckli and Vidale 2004). The NDVI parameter, estimator of the 'greenness' of the vegetation, mirrors the phenological state of the land cover, the 'greenness' of the vegetation obviously being related to leaf outburst and fall. The NDVI parameter is estimated from the red (RED) and near-infrared (NIR) information retrieved by the AVHRR sensor ($NDVI = (NIR - RED)/(NIR + RED)$).

Land surface phenology has been studied through temporal analyses of the NDVI parameter for various regions. A review of the methodologies applied by previous authors can be found in Julien and Sobrino (2009). Additionally, White *et al*. (2005) developed a framework for monitoring land surface phenological response to climate change. Suzuki *et al*. (2003, 2006) observed the timing of phenological events in northern Asia (Suzuki *et al*. 2003) and the relationship between the vegetation in this region and wetness and warmth indicators (Suzuki *et al*. 2006). De Beurs and Henebry (2004, 2005) combined the use of NDVI data with accumulated growing degree-days to observe structural changes in Kazakhstan (De Beurs and Henebry 2004) and interannual variation in the International Geosphere–Biosphere Program high-latitude transects (De Beurs and Henebry 2005). Karlsen *et al*. (2006) found that time-integrated NDVI values were highly correlated to growing degree-days in homogeneous areas of Fennoscandia. Delbart *et al*. (2005, 2006) and Delbart and Picard (2007) used the Normalized Difference Water Index (NDWI) to distinguish between snow influence and land surface phenology and linked its variations to air temperature in boreal areas. Heumann *et al*. (2007) related the observed variations and Soudan phenology to rainfall changes, while no significant trends could be identified in

the Sahel. Zhang *et al*. (2003) used Moderate Resolution Imaging Spectroradiometer (MODIS) data to retrieve land surface phenology with the help of piecewise logistic functions in north-eastern USA. By combining vegetation index and land surface temperature retrieved from the same sensor, Zhang *et al*. (2004) described the urban heat island effects as well as phenological phases for latitudes between 35°N and 70°N. Zhang *et al*. (2006) related these observations to *in situ* observations and temperature patterns.

This study aims at identifying trends in phenological spring dates at global scale from the analysis of air temperature records, which go back to 1948 and allow a better multi-temporal analysis than remotely sensed data, which go back only to the early 1980s. Of course, meteorological datasets have a lower spatial resolution than satellite datasets; however, they allow a first estimation of the trends.

To achieve this goal, we use the global spring dates retrieved from GIMMS data, in comparison with degree-day values for the same period, to identify the thresholds necessary to calculate the amount of degree-days reached at spring date. With the help of these thresholds, we then calculate the degree-day values for the second half of the twentieth century to finally estimate trends for phenological spring dates.

2. Data

Two different datasets are used in this study: the first consists of satellite images of vegetation index, while the second consists of meteorological modelled data – air temperatures.

2.1 *GIMMS data*

The GIMMS dataset (Pinzon 2002, Pinzon *et al*. 2004, Tucker *et al*. 2005) consists of NDVI images acquired by AVHRR on board NOAA satellites. This dataset is composed of bi-weekly composite images from July 1981 to December 2003, with a ground resolution of 8 km. The composite images are obtained by the Maximum Value Compositing (MVC) technique (Holben 1986), which minimizes the influence of atmospheric aerosols and clouds. The 22+ years of data were covered by five different satellites: NOAA-7, -9, -11, -14 and -16. NDVI images are obtained from AVHRR channel 1 and 2 images, which correspond, respectively, to red (0.58–0.68 μm) and infrared (0.73–1.1 μm) wavelengths.

This dataset, in spite of its limitation to NDVI data, presents several improvements regarding the Pathfinder AVHRR Land (PAL) dataset (Smith *et al*. 1997). The first improvement is a better data process, including navigation, sensor calibration and atmospheric correction for stratospheric aerosols. Another main improvement regards the correction of NOAA's orbital drift (Price 1991), through the empirical mode decomposition (EMD) technique (Pinzon *et al*. 2004).

Validity of the GIMMS dataset was discussed in previous studies (Zhou *et al*. 2001, Tucker *et al*. 2005) and, thus, is not assessed here. For our analysis, the whole dataset was used. GIMMS data were used indiscriminately of their flag attribute in order to dispose of the maximum number of pixels to cover the entire globe.

2.2 *Fifty-year Reanalysis*

This dataset was compiled by the National Center for Environmental Prediction (NCEP) and the National Center for Atmospheric Research (NCAR) and consists

of modelled meteorological data, from ground level to top of atmosphere, with various parameters, described in detail in Kalnay *et al*. (1996) and Kistler *et al*. (2001). For this study, only the data of air temperature at 2 m height were used.

These data were compiled from various sources (meteorological stations, buoys, airplane measurements and satellite images) and resampled through an assimilation system, to reach a temporal resolution of 6 hours and a spatial resolution of 2.5°. The dataset goes back to 1948 and is actualized regularly. In this study, all six-hourly 2 m air temperature data from 1948–2006 were used.

This dataset was preferred over Reanalysis II (Kanamitsu *et al*. 2002) and the ERA-40 dataset because it covered the longest period. The Reanalysis II dataset begins only in 1979 and, in spite of better data assimilation, does not expand significantly the time span covered by the GIMMS database. Assessment of the quality of the Reanalysis dataset can be found in Simmons *et al*. (2004) and Betts *et al*. (2006).

3. Method

A description of the fitting procedure applied to GIMMS data to retrieve spring dates is presented first, followed by an explanation of the degree-day calculation and ending with a description of the process to obtain the thresholds necessary for degree-day calculations. A flow chart of the method is presented in figure 1.

3.1 *Fitting procedure*

The method used to estimate the phenological dates of the vegetation is based on fitting NDVI data to a double logistic function (Beck *et al*. 2006) on a yearly basis. This

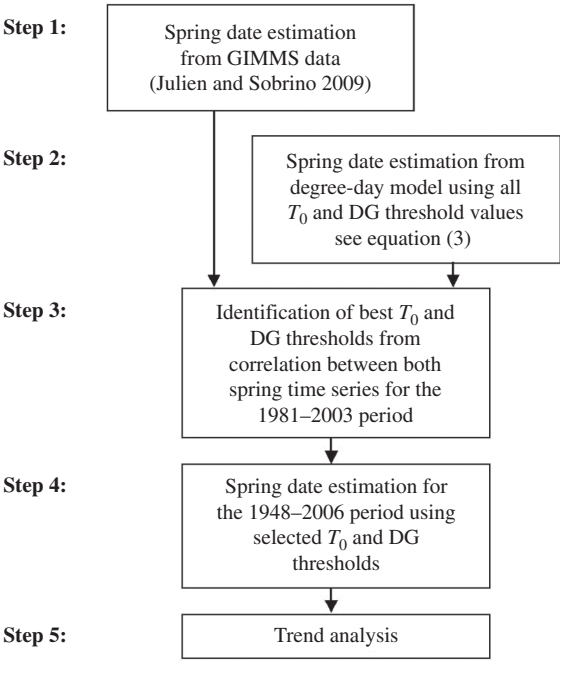

Figure 1. Flow chart of the procedure used to analyse trends in spring dates estimated from Reanalysis data using the degree-day model.

method is preferred over other methods (harmonic analysis, simple threshold determination) because of its ability to represent the vegetation seasonal cycle (adjustable dormancy period, growth peak or plateau). The fitting procedure is carried out using the Levenberg–Marquardt technique (More 1977) and a detailed description of its implementation can be found in Julien and Sobrino (2009), along with the representativeness of this double logistic fitting function for global vegetation monitoring. Trends obtained using this approach have been described and show good agreement with previous results (Julien and Sobrino 2009).

The double logistic function has the following expression:

$$\mathrm{NDVI}\,(t) = w_{\mathrm{NDVI}} + (m_{\mathrm{NDVI}} - w_{\mathrm{NDVI}}) \left(\frac{1}{1 + e^{-m_S \times (t-S)}} + \frac{1}{1 + e^{m_A \times (t-A)}} - 1 \right) \quad (1)$$

where NDVI(t) is the remotely sensed NDVI evolution for a given year at composite date t ($t = 0$ to 23), w_{NDVI} is the winter NDVI value, m_{NDVI} is the maximum NDVI value, S is the increasing inflection point (later referred to as spring date), A is the decreasing inflection point (autumn date) and m_S (respectively m_A) is related to the rate of increase (resp. decrease) at the S (resp. A) inflection point. In this equation, the spring date corresponds to the date at which the mid-point of the annual NDVI amplitude is reached and can be related to the onset of the vegetation. However, since the NDVI values corresponding to the actual leaf outburst vary as a function of plant species, these spring dates cannot be related directly to ground phenology.

Equation (1) describes more generally vegetation with photosynthetic peak activity around the middle of the year, with dormancy periods at the beginning and end of the year. However, it describes correctly the behaviour of most vegetation types, with the exception of those with two growing seasons during the year. The latter case exists only in a few areas (such as East Africa or the Indus River basin in Punjab, Pakistan) and represents less than 1% of the total amount of vegetated pixels (Julien and Sobrino 2009).

For a global study, satellite data were separated into hemisphere images following the Equator and, for the Southern Hemisphere, the same fitting procedure was applied, with the difference that the yearly data were compiled from 1 July to 30 June (instead of 1 January to 31 December for the Northern Hemisphere).

Biomes with photosynthetic peak activity at the boundary dates (around January or December), usually located in arid or semi-arid areas, are fitted to the following function:

$$\mathrm{NDVI}\,(t) = m_{\mathrm{NDVI}} - (m_{\mathrm{NDVI}} - w_{\mathrm{NDVI}}) \left(\frac{1}{1 + e^{-m_S \times (t-S)}} + \frac{1}{1 + e^{m_A \times (t-A)}} - 1 \right) \quad (2)$$

where all parameters are the same as for equation (1).

For biomes with low NDVI amplitude variation throughout the year (identified as the ones with an NDVI difference between maximum and minimum values lower than 0.1 NDVI unit), no fitting procedure is carried out in order to save computing time. In that case, no phenological phases are retrieved for the considered year. These biomes correspond to arid or frozen areas, as well as cloud-free evergreen vegetation.

The fitting procedure is carried out iteratively on a pixel-by-pixel basis for each of the 22 years available from the GIMMS database, using the Levenberg–Marquardt technique (More 1977). First, if NDVI time-series are below zero or with an amplitude

(difference between annual maximum and minimum) lower than 0.1, corresponding respectively, to frozen and stable areas, the pixel is flagged as such and no fitting procedure is carried out. Otherwise, a preliminary fit is conducted in order to choose between equations (1) and (2). Then, from this preliminary fit, the dormancy period is estimated as the period before the spring and after the autumn dates. During this dormancy period, all eventual negative NDVI values are set to the highest positive value over the whole dormancy period. Then, a weighted fit is carried out iteratively to the selected function (equation (1) or (2)), all NDVI values below the fitting function being considered as cloud-contaminated values and, thus, a lower weight is attributed to them for the next iteration. These weights are set to 1 for each date at the first iteration of the fitting procedure and then decreased by the difference between the data before and after the fit divided by the maximum NDVI value over the year for the dates flagged as cloudy (corresponding to lower NDVI values after the fit than before it). The procedure is stopped when the total difference between the weighted data and the fitting function is lower than 0.05 NDVI units. Finally, the fitting parameters are tested for consistency ($w_{\mathrm{NDVI}} \geq 0$, $m_{\mathrm{NDVI}} \leq 1$, $w_{\mathrm{NDVI}} \leq m_{\mathrm{NDVI}}$, $0 \leq S$ and $A \leq 365$, $S \leq A$ for equation (1) and $A \leq S$ for equation (2)). If these last tests are successful, the pixel is flagged as ok; if otherwise, it is flagged as unsuccessful.

In the case of standard biomes (one chlorophyll peak activity per year), the main source of inaccuracy in this procedure is due to the composite nature of the data. In order to estimate the accuracy in determining spring and autumn dates, a simulation was conducted, attributing randomly different acquisition dates for each 15-day period to a yearly time-series of data. Some 100 000 simulations were conducted, which led to standard deviations of ± 5.5 days of accuracy for spring dates (Julien and Sobrino 2009). These resulted from the lack of information of the chosen date for each pixel within a given NDVI composite, which is not provided with the GIMMS data.

Direct validation of the phenological phases from ground records is complicated due to the differences between datasets (White *et al*. 2005). One of these differences is obviously spatial resolution, since ground phenological datasets are dedicated to mainly a few species, while the chosen remotely sensed dataset averages species over the spatial extent of one pixel (64 km^2 along the Equator in the case of the satellite data used in this study). This is the reason why trend comparison with previous studies is usually carried out for validation purposes.

3.2 *Degree-days calculation*

Réaumur (1735) introduced degree-days as a descriptor of plant phenology. Each vegetal species has its own degree-day thresholds (Snyder *et al*. 1999) corresponding to specific development events (such as bud sprouting, blooming, fruit maturation and senescence) and degree-days are calculated with different thresholds depending on plant characteristics. The general formula for degree-day calculation is the following:

$$\mathrm{DG} = \sum_{T > T_0} (T - T_0) \tag{3}$$

where DG is the degree-day total amount, T corresponds to the daily averaged air temperature at 2 m (in °C) and T_0 to a temperature threshold depending on the plant characteristics (see table 1), the sum being calculated only for the days for which the

Table 1. Examples of T_0 threshold values for various plant species as retrieved from various authors.

T_0	Species	Publication
4.44	wheat, barley, rye, oats, flaxseed, lettuce, asparagus	Vaughn (2005)
7.22	sunflower, potato	Vaughn (2005)
10	sweetcorn, corn, sorghum, rice, soybeans, tomato	Vaughn (2005)
3.5	alfalfa	Sharratt *et al*. (1989)
9.4	citrus	Lovatt *et al*. (1984)
−2.04	bean PI 165-426	Scully and Waines (1988)
−4.48	bean Commodore	Scully and Waines (1988)
−1.9	bean Dark Red Kidney	Scully and Waines (1988)
−0.91	bean Linden	Scully and Waines (1988)
5.05	bean Black Turtle Soup	Scully and Waines (1988)
4.37	bean Sutter	Scully and Waines (1988)
6.4	bean Sal	Scully and Waines (1988)
6.17	bean Seedsaja	Scully and Waines (1988)
10	grapevine	Williams *et al*. (1985)
10	pistachio	Purcell and Welter (1991)
5.2	rose	Pasian and Lieth (1994)
10	sweetcorn	Coop *et al*. (1993)
7.21	tepary bean G40034	Scully and Waines (1988)
8.4	tepary bean Hood White	Scully and Waines (1988)
7.89	tepary bean G40016	Scully and Waines (1988)
0	winter wheat	McMaster and Smika (1988)
10	corn	Cross and Zuber (1972)
4.1(1 − 5.2)	deciduous forests in central Siberia	Delbart and Picard (2007)
0 − 5	all	Spano *et al*. (1999)

daily averaged air temperature at 2 m is higher than the given threshold (T_0), starting 1 January for the Northern Hemisphere and 1 July for the Southern Hemisphere. Daily averaged air temperatures (T) are calculated as averages of the four six-hourly air temperatures available from Reanalysis corresponding to the given day. Values of T_0 are plant dependent and vary as a function of plant species. Example of T_0 values for various species can be found in table 1. As shown, T_0 thresholds are highly dependent on plant type, which cannot be identified at the coarse resolution of the Reanalysis data. Therefore, we chose to use values of T_0 varying between 0 and 15°C with 1°C temperature steps. Degree-day annual amounts are an indicator of the climate and can be used for climatic area classification (Sobrino *et al*. 2006). However, the degree-day model for plant phenology is applicable only in areas where temperature is the limiting factor for plant growth, which is not the case in tropical areas, for example. The approach presented above was carried out at global scale to avoid limiting the study to the 45–75° N latitude band, with the aim of identifying the areas where this approach is valid. Such validity is discussed later.

3.3 *Thresholds retrieval*

The two datasets used in this study have different spatial resolutions; therefore, GIMMS-retrieved spring date images were resampled at Reanalysis resolution by identifying for each Reanalysis pixel the GIMMS pixel closer to its geolocation

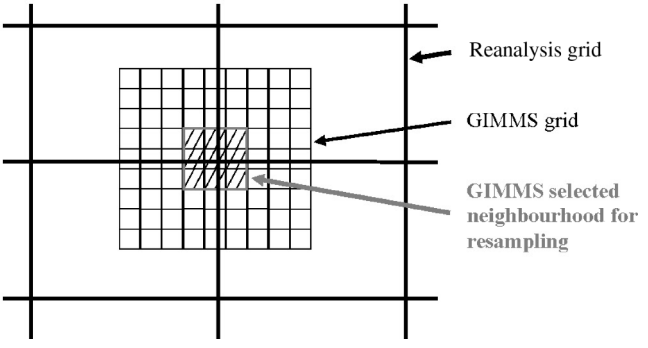

Figure 2. Schematic view of the resampling process between Reanalysis coarse data and the GIMMS NDVI grid.

(latitude and longitude). The spring date assigned to the resampled image is calculated from a 3×3 neighbourhood around this GIMMS pixel, over which valid spring dates are averaged (figure 2). This approach was chosen to avoid downscaling of the Reanalysis data, which would need additional information to be carried out satisfactorily, or to avoid interpolation of the Reanalysis data to the GIMMS resolution, which would both result in additional uncertainties in the data. Therefore, Reanalysis data were considered as describing locally the vegetation characterized with GIMMS 3×3 neighbouring pixels on a Reanalysis coarse grid.

Then, two thresholds have to be determined for each pixel: T_0, associated with the characteristics of the vegetation present in the considered pixel; and DG, amount of degree-days corresponding to spring (or leaf outburst), related both to vegetation and climate (see equation (3)). To this end, maps are created of the dates corresponding to the day at which each DG threshold between 0 and 7000 degree-days (with steps of 10 degree-days) is reached using T_0 values from 0 to 15°C with steps of 1°C in the calculations. Therefore, 7001×16 maps are obtained, which correspond to every possible value of the DG and T_0 thresholds within the selected range. From these maps, spring date time-series are extracted for each pixel and for every possible value of the T_0 and DG thresholds. Pearson correlations between the time-series of GIMMS-retrieved spring dates and the time-series of Reanalysis modelled spring dates are then calculated for all DG and T_0 values, and the DG and T_0 values corresponding to the highest Pearson correlations are selected as the adequate thresholds for degree-day calculations for this study. Pearson's correlation method was chosen since we expect the relation between satellite and degree-day estimated spring dates to be linear. Correlation is expected to reach significant values for temperature-limited vegetation (in temperate and boreal areas), since degree-day amounts are a common tool for determining their phenological phases. Of course, for vegetation limited by soil nutrients or water availability, correlation values are expected to be low. Due to the difference in the resolution of the datasets, the obtained T_0 and DG thresholds are not expected to correspond to specific plant species, although they should be representative of the land cover and the climate of the corresponding area. Since these thresholds are retrieved from the spring dates obtained from remotely sensed data, these thresholds are assumed to be constant through time, which implies an absence of change in the land cover. If land-cover change occurred during the 1981–2003 period, the threshold values for the affected pixels may be erroneous. Eventual changes in land

cover during the whole study (1948–2006) are not accounted for as regards threshold values. The approach is not sensitive to land-cover change in the 1948–2006 period, except if this land-cover change has been taken into account in the Reanalysis data through air temperature data assimilation.

Finally, with the help of these two thresholds, spring date time-series are calculated using equation (3) for the whole Reanalysis database (1948–2006) and then tested for trends using Mann–Kendall trend tests (Hirsch and Slack 1984, Julien and Sobrino 2009).

4. Results

Figure 3 shows the resampled spring date for 1990 in the Northern Hemisphere and 1990–1991 for the Southern Hemisphere. Those years have been chosen arbitrarily for display, although spring 1990 was recorded as the earliest ever in most of central and northern Europe (Menzel 2000, Chmielewski and Rötzer 2002, Karlsen *et al*. 2007). In boreal and temperate areas of the Northern Hemisphere, one can observe easily the latitudinal gradient in spring dates, the spring dates getting earlier at lower latitudes. This pattern does not show for the Indian subcontinent and the tropical areas, which can be explained easily by the special rain regimes that affect these areas.

Figure 4 presents the significance of the maximum values of the Pearson correlation obtained between time-series of GIMMS- and Reanalysis-retrieved spring dates for all DG and T_0 values for each pixel. These correlations are significant at the 95% level for correlations higher than 0.42 and at the 99% level for correlations higher than 0.54. From figure 4, one can observe that the pixels with the highest level of significance (99%) are located almost only in the northern temperate and boreal areas. Tropical and equatorial areas exhibit lower significance values. Figure 4 shows the areas for which the degree-day approach can be considered as valid ($p > 95\%$) and, therefore, a mask corresponding to confidence levels higher than 95% was applied to the following results. This mask includes 63% of the pixels corresponding to land and 74% of the pixels for which the double logistic fitting procedure was carried out.

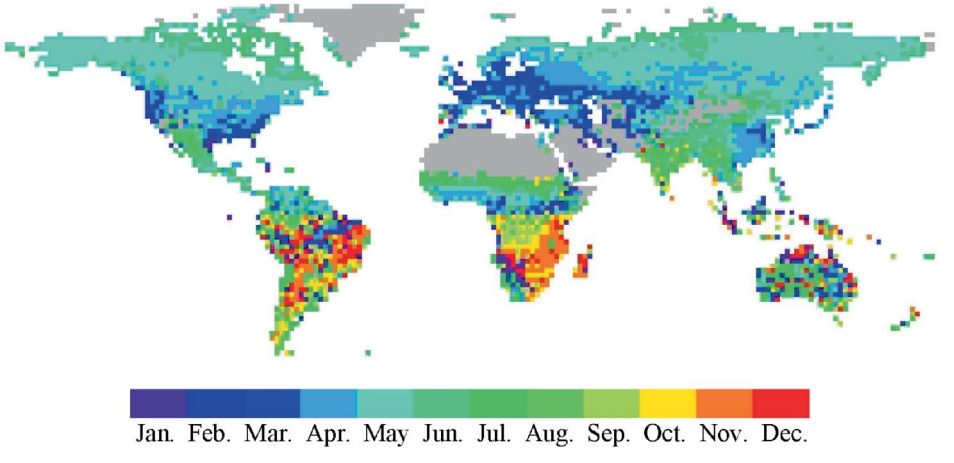

Figure 3. Spring dates for the year 1990 (Northern Hemisphere) and 1990–1991 (Southern Hemisphere) retrieved from GIMMS data.

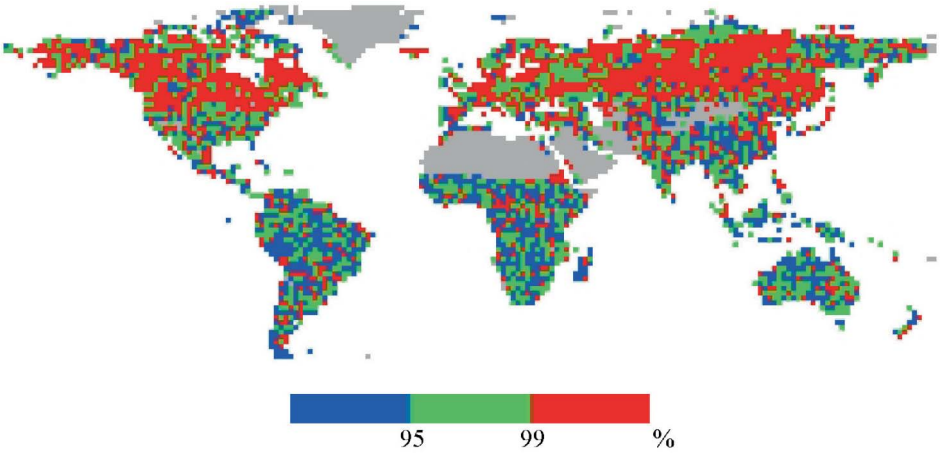

Figure 4. Level of significance (in percentage) for correlation values in threshold determination for degree-day calculations.

Figure 5 shows the spatial repartition of T_0 and DG thresholds around the globe (see equation (3)), only for those pixels with significant correlation values at the 95% confidence level. The T_0 threshold appears to be vegetation dependent, the polar areas tending to have a lower T_0 threshold with local exceptions, due mainly to land-cover type. T_0 shows a great spatial variability, probably due to land occupation (Snyder *et al*. 1999). This spatial variability in T_0 values is higher in tropical areas where vegetation is not temperature limited. DG thresholds show a latitudinal gradient, as expected, having a lower value near the poles and a higher value at low latitudes, with the exception of equatorial areas (see figure 5(*b*)). In these latter areas, spatial consistency may be altered by the fact that the vegetation is not temperature limited and by the presence of enduring cloud cover, which degrades the precision of spring determination in GIMMS images.

Figure 6(*a*) shows an example of spring date images for 1990 in the Northern Hemisphere and 1990–1991 for the Southern Hemisphere, both calculated from degree-days amounts, as well as the bias in spring date estimation when using the degree-day approach (figure 6(*b*)). By comparing this image with figure 3, one can observe that the spring dates for figure 6 occur globally sooner than for figure 3, especially in low latitudes, corresponding to the noisy area mentioned in figure 5(*b*).

Figure 7(*a*) presents the global trends obtained from the degree-day approach for the 1948–2006 period, showing only the trends (retrieved by ordinary least-square method) for the pixels passing Mann–Kendall trend tests at the 90% confidence level. The average trend for all the statistically significant values is around –0.03 days per year, which corresponds to almost a two-day overall advance in spring dates at a global scale over the past 59 years, with values ranging mainly from less than −0.9 days per year (advance) in Southern Africa and around the Himalayan mountains to more than +0.9 days per year (delay) along the Andes. Temperate areas, generally, see an advance in their Reanalysis-retrieved spring dates, corresponding to the well-documented increase in air temperature (IPCC 2007). Strong advances (greater than −0.5 days per year) are located mainly in mountains of the temperate areas, while strong delays (greater than +0.5 days per year) are located mainly in the Southern Hemisphere.

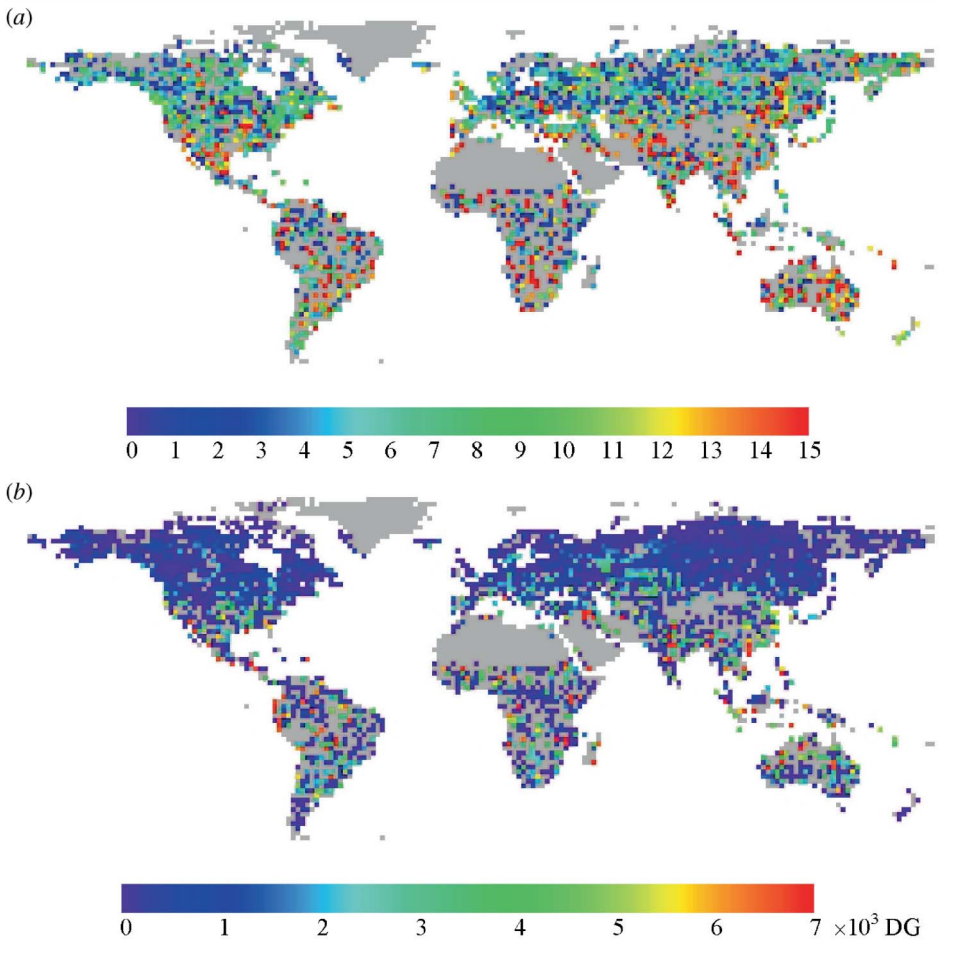

Figure 5. Retrieved thresholds for spring date estimation from degree-days: (*a*) T_0 – daily threshold (in °C); (*b*) DG – total degree-day amount (cf. equation (3)).

5. Discussion

The results presented above are in concordance with the well-documented increase in air temperature, which is part of the climatic change under way (IPCC 2007). However, the results presented here are based on a fitting technique on yearly satellite images, which, in spite of the compositing technique used, can include cloud-contaminated images, especially in areas with high cloud coverage, such as equatorial areas. The repeated presence of clouds influences the accuracy of the determination of spring dates, which in return provokes artificial instability in temporal series of spring dates (Julien and Sobrino 2009). This instability, in return, hinders the threshold estimations for degree-day calculations, since the correlation between the dates for reached degree amounts and spring dates is then diminished. However, trends retrieved by this approach were validated by comparison with numerous previous studies using satellite data as well as studies using phenological records or climate data (Julien and Sobrino 2009).

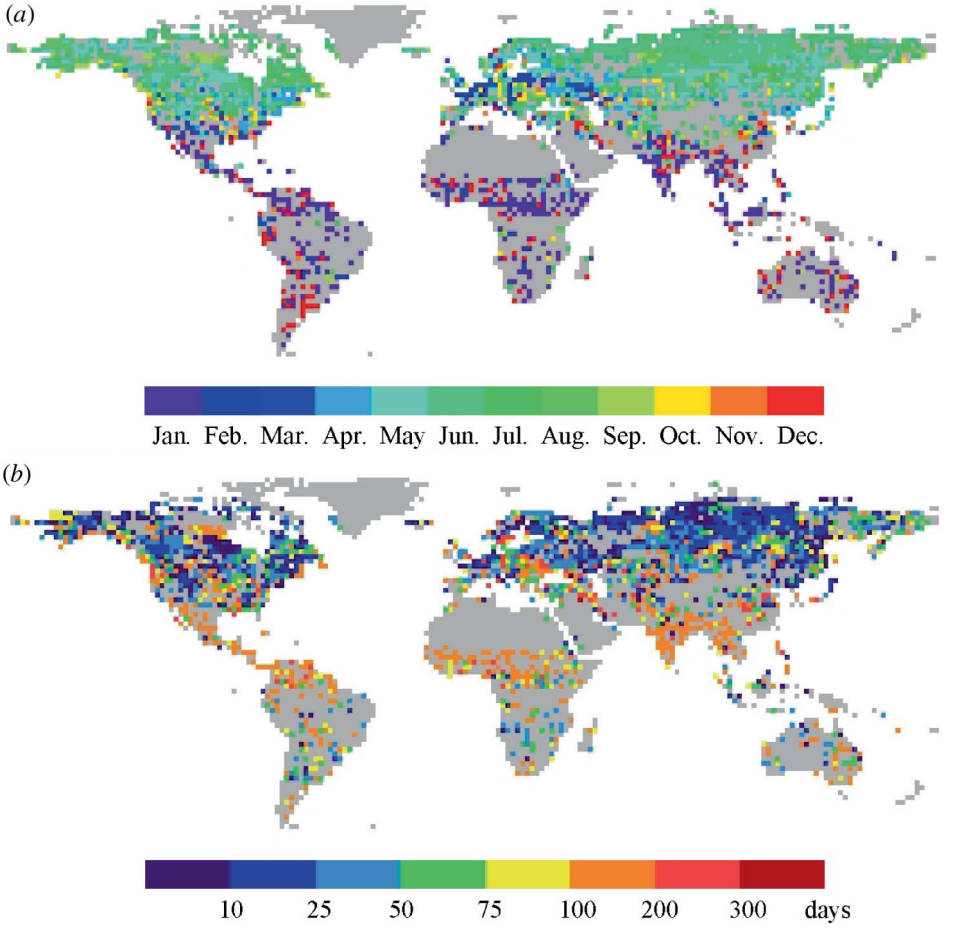

Figure 6. (*a*) Spring dates for the year 1990 (Northern Hemisphere) and 1990–1991 (Southern Hemisphere) estimated from degree-day amounts; and (*b*) bias in spring date estimation from the degree-day approach in comparison to the spring dates estimated from GIMMS data in days.

The differences between satellite and degree-day estimated spring dates (figure 7(*b*)) may seem quite important, although one has to keep in mind that the temporal resolution of satellite data is of the order of 15 days, while 50-year Reanalysis data are obtained on a daily basis. The lowest error is obtained for boreal and temperate areas, where vegetation is constrained more by temperatures than by other parameters (see figure 8), while the areas with lower NDVI amplitudes show higher errors. Therefore, figure 6(*b*) shows that the degree-day approach is not valid in areas where vegetation is not temperature limited, such as semi-arid areas and evergreen vegetation.

The approach chosen here supposes that the land cover of each studied pixel has not changed during the study period. This may not be the case; however, the implications of this hypothesis on the resulting trends are low. Although land-use change obviously contributes to phenology changes, it has a low probability of appearing as a significant trend in the data, since the observed changes are more likely to be abrupt in time (from one year to the other) and, therefore, decrease the significance of the observed trends.

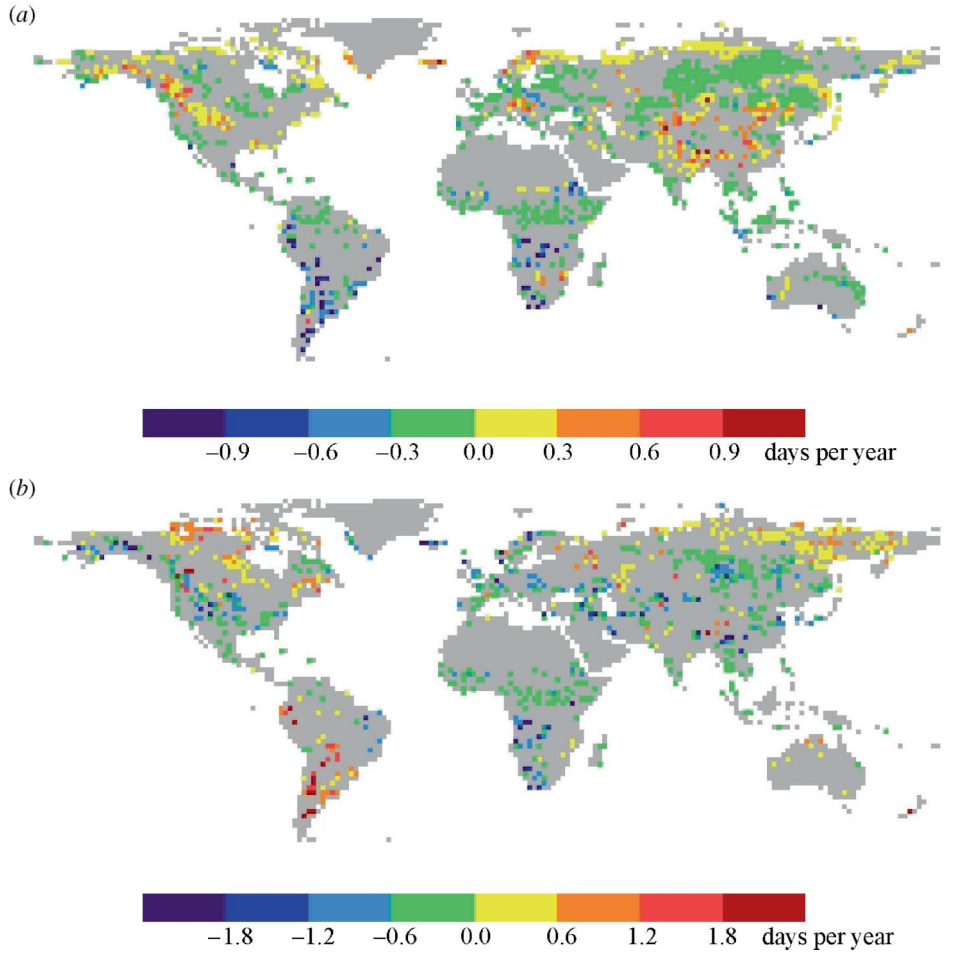

Figure 7. Trends for spring dates (in days per year) estimated from degree-day amounts for the 1948–2006 period (up) and for the 1981–2006 period (down). Only statistically meaningful trends (Mann–Kendall trend tests) are shown.

Julien and Sobrino (2009) have compiled phenological changes from various previous studies based on phenological, satellite and climate data. Many of these studies were carried out at the local or regional scale, which cannot be easily compared with our study due to the coarse resolution of the database used here (2.5°), leading to a small number of pixels for each considered country. The results presented above differ from previous studies (Myneni *et al*. 1997, Tucker *et al*. 2001, Zhou *et al*. 2001, Stöckli and Vidale 2004) in the fact that some areas (mainly boreal and mountainous areas of the Northern Hemisphere) see a delay in their spring phenology, a fact which does not appear in the mentioned studies. This can be due to the fact that the results are usually averaged on local to regional areas, when the approach described in this study is pixel-based. Moreover, only pixels with a statistically significant trend are considered here, meaning that all pixels with trends statistically insignificant at the 90% confidence level are rejected, when other studies usually average the estimated trends over a geographical area to, in a few cases, estimate the statistical significance of the results.

Trends for large areas (global, Northern Hemisphere, 45–75°N latitude band) obtained from satellite data usually have an estimated spring trend around –0.2 to −0.3 days per year (Myneni *et al*. 1997, Tucker *et al*. 2001, Zhou *et al*. 2001, Stöckli and Vidale 2004), which is higher than the results presented here (–0.03 days per year), although these global studies have been carried out from satellite data only, which never covers more than the last 25 years. When restricted to the period 1981–2006, the global average trend for this study increases to –0.09 days per year, closer to the values obtained in previous studies (see figure 7(*b*)).

A few phenological studies were conducted over large areas (Menzel and Fabian 1999, Ahas *et al*. 2002, Schwartz *et al*. 2006). Retrieved trends in first leaf dates range from +0.4 days per year over Eastern Europe to –1.0 days per year over Central and Western Europe (Ahas *et al*. 2002), while the average trend over Europe is –0.2 days per year (Menzel and Fabian 1999). Goetz *et al*. (2005) showed that nearly 15% of boreal North America displayed significant trends in vegetation activity between 1981 and 2003, divided almost equally between positive and negative trends. A similar proportion can be observed for our results in this area (see figure 7(*b*)). Reed (2006) showed that over the same period spring dates advanced for selected areas of the United States, which is also in agreement with the results presented in figure 7(*b*)). Over the Northern Hemisphere, the phenological trend in first leaf date is –0.12 days per year (Schwartz *et al*. 2006). These trends are more scattered than the ones retrieved from satellite data, due to the low coverage of phenological stations, with areas excluded from the study (like boreal and tropical areas). Nevertheless, the results presented here are within the order of magnitude of these trends.

Of course, the model used here takes into account only air temperature, without studying the influence of other parameters, such as available water, for example. Nemani *et al*. (2003) published a global map of climatic constraints to plant growth (their figure 1(a)). This map shows that plant growth is limited by temperature (at least partially) only in temperate and polar areas. These are the areas that are described correctly with the use of degree-days (as shown in figure 4), while the rest of the globe would need the inclusion of precipitation to complete the model. One can observe that the temperate and polar areas are the ones showing the higher concentration of low confidence levels for correlation values between satellite and degree-day estimates of the spring date in figure 4.

Moreover, the Reanalysis model is known to behave badly around mountains, where high spatial variability cannot be described correctly by its 2.5° grid. Mountainous areas are actually the ones showing the highest trend values (positive as well as negative) for both the 1948–2006 and 1981–2006 periods. For the 1981−2006 period, the highest delays (+1.8 days per year) in the spring occurrence are obtained around the Andes mountains, while for the 1948–2006 period, the highest delays (+0.9 days per year) in the spring occurrence are obtained around the Rocky and Himalaya mountains, while some pixels in the Andes mountains show the highest advances (–0.9 days per year). The inverse trend pattern around the Andes for the 1948–2006 and 1981–2006 periods is highly suspicious and would need some direct comparison with phenological ground data for validation. However, the authors could not find any regional or continental phenological record for direct comparison.

6. Conclusion

This study has used the whole GIMMS dataset to determine phenological spring dates, from which phenological degree-day thresholds were estimated. These

thresholds allow for the calculation of spring dates from meteorological data, namely the 2 m height air temperature from the Reanalysis database. This study has thus extended phenological results from satellite data, limited to the past 25 years, to meteorological data, which go back to the past 60 years.

Moreover, this study has analysed trends in spring phenology, which on average have a value of –0.03 days per year for the 1948–2006 period, which represents an advance of almost two days over the 58-year study period. Trends in spring dates are included between −0.9 and +0.9 days per year (corresponding respectively to advances and delays of 52 days over the whole data period). The described trends are smaller than the ones presented in previous studies, a fact that can be explained by the difference in the database time span and by the fact that the Southern Hemisphere is usually ignored.

Thus, this work has shown the possibility of extending results obtained by remote sensing techniques back into the past with the help of air temperature for areas with vegetation limited by temperature, in order to obtain almost 60 years of land surface phenology. Comparison with the results of previous studies has validated this approach and the retrieved spring dates could be compared to historical phenological ground records in order to improve characterization of climate change influence on vegetation.

Acknowledgements

The authors wish to thank the European Union EAGLE project (SST3-CT-2003-502057) and the TERMASAT project (Ministerio de Educación y Ciencia, project ESP2005-07724-C05-04) for financial support. The source for the data used in this work was the Global Land Cover Facility.

References

Ahas, R., Aasa, A., Menzel, A., Fedotova, V.G. and Scheifinger, H., 2002, Changes in European spring phenology. *International Journal of Climatology*, **22**, pp. 1727–1738.

Beck, P., Atzberger, C., Hogda, K.A., Johansen, B. and Skidmore A., 2006, Improved monitoring of vegetation dynamics at very high latitudes: a new method using MODIS NDVI. *Remote Sensing of Environment*, **100**, pp. 321–334.

Betts, A.K., Zhao, M., Dirmeyer, P.A. and Beljaars, A.C.M., 2006, Comparison of ERA-40 and NCEP/DOE near-surface data sets with other ISLSCP-II data sets. *Journal of Geophysical Research*, **11**, D22S04, doi: 10.1029/2006JD007174.

Bogaert, J., Zhou, L., Tucker, C.J., Myneni, R.B. and Ceulemans, R., 2002, Evidence for a persistent and extensive greening trend in Eurasia inferred from satellite vegetation index data. *Journal of Geophysical Research*, **107**, doi: 10.1029/2001JD001075.

Chen, X., Hu, B. and Yu, R., 2005, Spatial and temporal variation of phenological growing season and climate change impacts in temperate eastern China. *Global Change Biology*, **11**, pp. 1118–1130.

Chmielewski, F.-M. and Rötzer, T., 2002, Annual and spatial variability of the beginning of growing season in Europe in relation to air temperature changes. *Climate Research*, **19**, pp. 257–264.

Coop, L.B., Croft, B.A. and Drapek, R.J., 1993, Model of corn earworm (Lepidoptera: Noctuidae) development, damage, and crop loss in sweet corn. *Journal of Economic Entomology*, **86**, pp. 906–916.

Cross, H.Z. and Zuber, M.S., 1972, Prediction of flowering dates in maize based on different methods of estimating thermal units. *Agronomy Journal*, **64**, pp. 351–355.

De Beurs, K.M. and Henebry, G.M., 2004, Land surface phenology, climatic variation, and institutional change: analyzing agricultural land cover change in Kazakhstan. *Remote Sensing of Environment*, **89**, pp. 497–509.

De Beurs, K.M. and Henebry, G.M., 2005, Land surface phenology and temperature variation in the International Geosphere–Biosphere Program high-latitude transects. *Global Change Biology*, **11**, pp. 779–790.

Delbart, N., Kergoat, L., Le Toan, T., Lhermitte, J. and Picard, G., 2005, Determination of phenological dates in boreal regions using normalized difference water index. *Remote Sensing of Environment*, **97**, pp. 26–38.

Delbart, N., Le Toan, T., Kergoat, L. and Fedotova, V., 2006, Remote sensing of spring phenology in boreal regions: a free of snow-effect method using NOAA-AVHRR and SPOT-VGT data (1982–2004). *Remote Sensing of Environment*, **101**, pp. 52–62.

Delbart, N. and Picard, G., 2007, Modeling the date of leaf appearance in low-arctic tundra. *Global Change Biology*, **13**, pp. 2551–2562.

Goetz, S.J., Bunn, A.G., Fiske, G.J. and Houghton, R.A., 2005, Satellite-observed photosynthetic trends across boreal North America associated with climate and fire disturbance. *Proceedings of the National Academy of Sciences of the United States of America*, **102**, pp. 13521–13525.

Green, R.E., Harley, M., Miles, L., Scharlemann, J., Watkinson, A. and Watts, O., (Eds), 2003, *Conference on Global Climate Change and Biodiversity*, April, University of East Anglia, Norwich, UK.

Heumann, B.W., Seaquist, J.W., Eklundh, L. and Jönsson, P., 2007, AVHRR derived phenological change in the Sahel and Soudan, Africa, 1982–2005. *Remote Sensing of Environment*, **108**, pp. 385–392.

Hirsch, R.M. and Slack, J.R., 1984, A nonparametric trend test for seasonal data with serial dependence. *Water Resources Research*, **20**, pp. 727–732.

Holben, B.N., 1986, Characteristics of maximum values composite images from temporal AVHRR data. *International Journal of Remote Sensing*, **7**, pp. 1417–1434.

IPCC, 2007, *Climate Change 2007: Impacts, Adaptation, and Vulnerability*. Contribution of Working Group II to the Fourth Assessment Report of the Intergovernmental Panel on Climate Change, M.L. Parry, O.F. Canziani, J.P. Palutikof, P.J. van der Linden and C.E. Hanson (Eds) (Cambridge: Cambridge University Press).

Julien, Y. and Sobrino, J.A., 2009, Global land surface phenology trends from GIMMS database. *International Journal of Remote Sensing*, **30**, pp. 3495–3513.

Kalnay, E., Kanamitsu, M., Kistler, R., Collins, W., Gandin, L., Iredell, M., Saha, S., White, G., Woollen, J., Zhu, Y., Chelliah, M., Ebisuzaki, W., Higgins, W., Janowiak, J., Mo, K.C., Ropelewski, C., Wang, J., Leetmaa, A., Reynolds, R., Jenne, R. and Joseph, D., 1996, The NCEP/NCAR 40-Year Reanalysis Project. *Bulletin of the American Meteorology Society*, **77**, pp. 3427–3471.

Kanamitsu, M., Ebisuzaki, W., Woollen, J., Yang, S.-K., Hnilo, J.J., Fiorino, M. and Potter, G.L., 2002, NCEP-DOE AMIP-II REANALYSIS (R-2). *Bulletin of the American Meteorological Society*, **83**, pp. 1631–1643.

Karlsen, S.R., Elveball, A., Høgda, K.A. and Johansen, B., 2006, Satellite-based mapping of the growing season and bioclimatic zones in Fennoscandia. *Global Ecology and Biogeography*, **15**, pp. 416–430.

Karlsen, S.R., Solheim, I., Beck, P.S.A., Høgda, K.A., Wielgolaski, F.E. and Tømmervik, H., 2007, Variability of the start of the growing season in Fennoscandia, 1982–2002. *International Journal of Biometeorology*, **51**, pp. 513–524.

Kistler, R., Kalnay, E., Collins, W., Saha, S., White, G., Woollen, J., Chelliah, M., Ebisuzaki, W., Kanamitsu, M., Kousky, V., van den Dool, H., Jenne, R. and Fiorino, M., 2001, The NCEP-NCAR 50-Year Reanalysis: monthly means CD-ROM and documentation. *Bulletin of the American Meteorology Society*, **82**, pp. 247–267.

Lovatt, C.J., Streeter, S.M., Minter, T.C., O'Connell, N.V., Flaherty, D.L., Freeman, M.W. and Goodell, P.B., 1984, Phenology of flowering in *Citrus sinensis* [L.] Osbeck, cv. Washington Naval orange. *Proceedings of the International Society of Citriculture*, **1**, pp. 186–190.

McMaster, G.S. and Smika, D.E., 1988, Estimation and evaluation of winter wheat phenology in the central Great Plains. *Agricultural and Forest Meteorology*, **60**, pp. 193–220.

Menzel, A., 2000, Trends in phenological phases in Europe between 1951 and 1996. *International Journal of Biometeorology*, **44**, pp. 76–81.

Menzel, A. and Fabian, P., 1999, Growing season extended in Europe. *Nature*, **397**, p. 659.

More, J.J., 1977, The Levenberg–Marquardt algorithm: implementation and theory. In *Numerical Analysis*, Lecture Notes in Mathematics 630, G.A. Watson (Ed.), pp. 105–116 (Berlin: Springer-Verlag).

Myneni, R.B., Keeling, C.D., Tucker, C.J., Asrar, G. and Nemani, R.R., 1997, Increased plant growth in the northern high latitudes from 1981 to 1991. *Nature*, **386**, pp. 698–702.

Nemani, R.R., Keeling, C.D., Hashimoto, H., Jolly, W.M., Piper, S.C., Tucker, C.J., Myneni, R.B. and Running, S.W., 2003, Climate-driven increases in global terrestrial net primary production from 1982 to 1999. *Science*, **300**, pp. 1560–1563.

Pasian, C.C. and Lieth, J.H., 1994, Prediction of flowering rose shoot development based on air temperature and thermal units. *Scientia Horticulturae*, **59**, pp. 131–145.

Pinzon, J., 2002, Using HHT to successfully uncouple seasonal and interannual components in remotely sensed data. In *SCI 2002 Conference Proceedings*, 14–18 July, Orlando, FL.

Pinzon, J., Brown, M.E. and Tucker, C.J., 2004, Satellite time series correction of orbital drift artifacts using empirical mode decomposition. In *EMD and Its Applications*, Vol. 10, N.E. Huang and S.S.P. Shen (Eds), pp. 285–295 (Singapore: World Scientific).

Price, J.C., 1991, Timing of NOAA afternoon passes. *International Journal of Remote Sensing*, **12**, pp. 193−198.

Purcell, M. and Welter, S.C., 1991, Effect of *Calocoris norvegicus* (Hemiptera: Miridae) on pistachio yields. *Journal of Economic Entomology*, **84**, pp. 114–119.

Réaumur, R.-A.F. de, 1735, Observations du thermomètre. *Mémories de l'Académie Royale des Sciences, Paris*, pp. 737–754.

Reed, B.C., 2006, Trend analysis of time-series phenology of North America derived from satellite data. *GIScience & Remote Sensing*, **43**, pp. 24–38.

Salinger, M.J., 2005, Climate variability and change: past, present and future – an overview. *Climatic Change*, **70**, pp. 9–29.

Schwartz, M.D., Ahas, R. and Aasa, A., 2006, Onset of spring starting earlier across the Northern Hemisphere. *Global Change Biology*, **12**, pp. 343–351.

Scully, B. and Waines, J.G., 1988, Ontogeny and yield response of common and tepary beans to temperature. *Agronomy Journal*, **80**, pp. 921–925.

Sharratt, B.S., Sheaffer, C.C. and Baker, D.G., 1989, Base temperature for the application of the growing-degree-day model to field-grown alfalfa. *Field Crops Research*, **21**, pp. 95–102.

Sherry, R.A., Zhou, X., Gu, S., Arnone III, J.A., Schimel, D.S., Verburg, P.S., Wallace, L.L. and Luo, Y., 2007, Divergence of reproductive phenology under climate warming. *PNAS*, **104**, pp. 198–202.

Simmons, A.J., Jones, P.D., da Costa Bechtold, V., Beljaars, A.C.M., Kållberg, P.W., Saarinen, S., Uppala, S.M., Viterbo, P. and Wedi, N., 2004, Comparison of trends and low-frequency variability in CRU, ERA-40, and NCEP/NCAR analyses of surface air temperature, *Journal of Geophysical Research*, **109**, D24115, doi: 10.1029/2004JD005306.

Smith, P.M., Kalluri, S.N.V., Prince, S.D. and Defries, R., 1997, The NOAA/NASA pathfinder AVHRR 8-km land data set. *Photogrammetric Engineering and Remote Sensing*, **63**, pp. 12–31.

Snyder, R.L., Spano, D., Cesaraccio, C. and Duce, P., 1999, Determining degree-day thresholds from field observations. *International Journal of Biometeorology*, **42**, pp. 177–182.

Sobrino, J.A., Julien, Y. and Morales, L., 2006, Multitemporal analysis of PAL images for the study of land cover dynamics in South America. *Global and Planetary Change*, **51**, pp. 172–180.

Spano, D., Cesaraccio, C., Duce, P. and Snyder, R.L., 1999, Phenological stage of natural species and their use as climate indicators. *International Journal of Biometeorology*, **42**, pp. 124–133.

Stöckli, R. and Vidale, P.L., 2004, European plant phenology and climate as seen in a 20-year AVHRR land-surface parameter dataset. *International Journal of Remote Sensing*, **25**, pp. 3303–3330.

Suzuki, R., Nomaki, T. and Yasunari, T., 2003, West–east contrast of phenology and climate in northern Asia revealed using a remotely sensed vegetation index. *International Journal of Biometeorology*, **47**, pp. 126–138.

Suzuki, R., Xu, J. and Motoya, K., 2006, Global analyses of satellite-derive vegetation index related to climatological wetness and warmth. *International Journal of Climatology*, **26**, pp. 425–438.

Tucker, C.J., Pinzon, J.E., Brown, M.E., Slayback, D.A., Pak, E.W., Mahoney, R., Vermote, E.F. and El Saleous, N., 2005, An extended AVHRR 8-km NDVI dataset compatible with MODIS and SPOT vegetation NDVI data. *International Journal of Remote Sensing*, **26**, pp. 4485–4498.

Tucker, C.J., Slayback, D.A., Pinzon, J.E., Los, S.O., Myneni, R.B. and Taylor, M.G., 2001, Higher northern latitude NDVI and growing season trends from 1982 to 1999. *International Journal of Biometeorology*, **45**, pp. 184–190.

Vaughn, D.M., 2005, Degree days. In *Encyclopedy of World Climate*, J.E. Oliver (Ed.), pp. 336–339 (Berlin: Springer-Verlag).

Weber, K.T., 2001, A method to incorporate phenology into land cover change analysis. *Journal of Range Management*, **54**, pp. A1–A7.

White, M.A., Hoffman, F., Hargrove, W.W. and Nemani, R.R., 2005, A global framework for monitoring phenological responses to climate change. *Geophysical Research Letters*, **32**, L04705, doi: 10.1029/2004GL021961.

Williams, D.W., Andris, H.L., Beede, R.H., Luvisi, D.A., Norton, M.V.K. and Williams, L.E., 1985, Validation of a model for the growth and development of the Thompson seedless grapevine. II. Phenology. *American Journal of Enology and Viticulture*, **36**, pp. 283–289.

Zhang, X., Friedl, M.A. and Schaaf, C.B., 2006, Global vegetation phenology from moderate resolution imaging spectroradiometer (MODIS): evaluation of global patterns and comparison with in situ measurements. *Journal of Geophysical Research*, **111**, G04017, doi: 10.1029/2006JG000217.

Zhang, X., Friedl, M.A., Schaaf, C.B. and Strahler, A.H., 2004, Climate controls on vegetation phenological patterns in northern mid- and high latitudes inferred from MODIS data. *Global Change Biology*, **10**, pp. 1133–1145.

Zhang, X., Friedl, M.A., Schaaf, C.B., Strahler, A.H., Hodges, J.C.F., Gao, F., Reed, B.C. and Huete, A., 2003, Monitoring vegetation phenology using MODIS. *Remote Sensing of Environment*, **84**, pp. 471–475.

Zhou, L., Tucker, C.J., Jaufmann, R.K., Slayback, D., Shabanov, N.V. and Myneni, R.B., 2001, Variations in northern vegetation activity inferred from satellite data of vegetation index during 1981 to 1999. *Journal of Geophysical Research*, **106**, pp. 20 069–20 083.